ORNL-4960

TRANSIENT RESPONSE OF LOW FREQUENCY VERTICAL ANTENNAS TO HIGH ALTITUDE NUCLEAR ELECTROMAGNETIC PULSE (EMP)

P. R. Barnes
D. B. Nelson

BLANK PAGE

Printed in the United States of America. Available from
National Technical Information Service
U.S. Department of Commerce
5285 Port Royal Road, Springfield, Virginia 22151
Price: Printed Copy $4.00; Microfiche $0.95

ORNL-4960
UC-2 – General, Miscellaneous,
and Progress Reports

HEALTH PHYSICS DIVISION

Civil Defense Research Section

TRANSIENT RESPONSE OF LOW FREQUENCY VERTICAL ANTENNAS TO HIGH ALTITUDE NUCLEAR ELECTROMAGNETIC PULSE (EMP)*

P. R. Barnes and D. B. Nelson

JUNE 1974

*Research sponsored by the Air Force Weapons Laboratory under Union Carbide Corporation's contract with the U.S. Atomic Energy Commission.

OAK RIDGE NATIONAL LABORATORY
Oak Ridge, Tennessee 37830
operated by
UNION CARBIDE CORPORATION
for the
U.S. ATOMIC ENERGY COMMISSION

TABLE OF CONTENTS

LIST OF FIGURES

TRANSIENT RESPONSE OF LOW FREQUENCY VERTICAL ANTENNAS TO HIGH ALTITUDE NUCLEAR ELECTROMAGNETIC PULSE (EMP)

P. R. Barnes and D. B. Nelson

ABSTRACT

Several antenna models are used to calculate the transient response of top-loaded LF vertical antennas to EMP from high altitude nuclear detonations. Examples are given of the short circuit current and voltage across an idealized load for a 360 meter high, top-loaded antenna illuminated by two representative EMP fields. Good agreement is obtained among all the models used.

The effect of the angle of incidence θ is quite pronounced. The early time current and voltage at 30° is almost twice what it is at 90°, confirming the $\sin^{-1}\theta$ behavior. On the other hand, end effects occur sooner at 30°, reducing the low frequency content. Thus the late time behavior is largest at 90°. In general it will be true for long antennas that effects depending on initial rate of rise will be maximized for small θ, whereas effects that depend on total surge energy are maximized for broadside incidence.

1. INTRODUCTION

1.1 Purpose and Content

This report has been prepared for two purposes: first, to exhibit methods for calculating the response to transient electromagnetic waves of long thin antennas used for low frequency (LF) radio transmission; and second, to give examples of the surge currents and voltages induced in such antennas and their coupling circuits by the electromagnetic pulse (EMP) from high altitude nuclear detonations.

Because LF monopoles are normally several hundred meters tall, they are electrically long for much of the EMP spectrum. Accordingly, many antenna resonances must be included to compute the response accurately. Because the models used describe the antenna in the frequency domain, with time domain answers given via an inverse Laplace or Fourier transform, a wide range of frequencies is required. To assure that correct results are obtained we have employed several theoretical models valid in different regions and have compared results in the overlapping regions of validity. The simplest of these is the semi-infinite cylindrical antenna erected perpendicular to an infinite ground plane;[1] this model gives valid results until the first end reflection reaches the point of interest. For later times the finite length antenna must be considered. Two different models are used in this regime. The first of these is a classical theory of the monopole, using the work of King[2] for the electrically short antenna and of Wu[3] for the long antenna. (We have also used a modification of this due to Shen, Wu, and King.[4,5]) The second is the singularity expansion method, developed by Baum[6] and applied to the cylindrical dipole and monopole antennas by Barnes.[7] This application of the singularity expansion method is presently developed for broadside wave incidence (electric field parallel to the antenna) but it is easy to compute and gives good results for late time. The classical method is the more powerful, in principle giving results for all time and all angles of incidence. In practice, its reliance on a brute force Fourier transform along the real frequency axis makes it

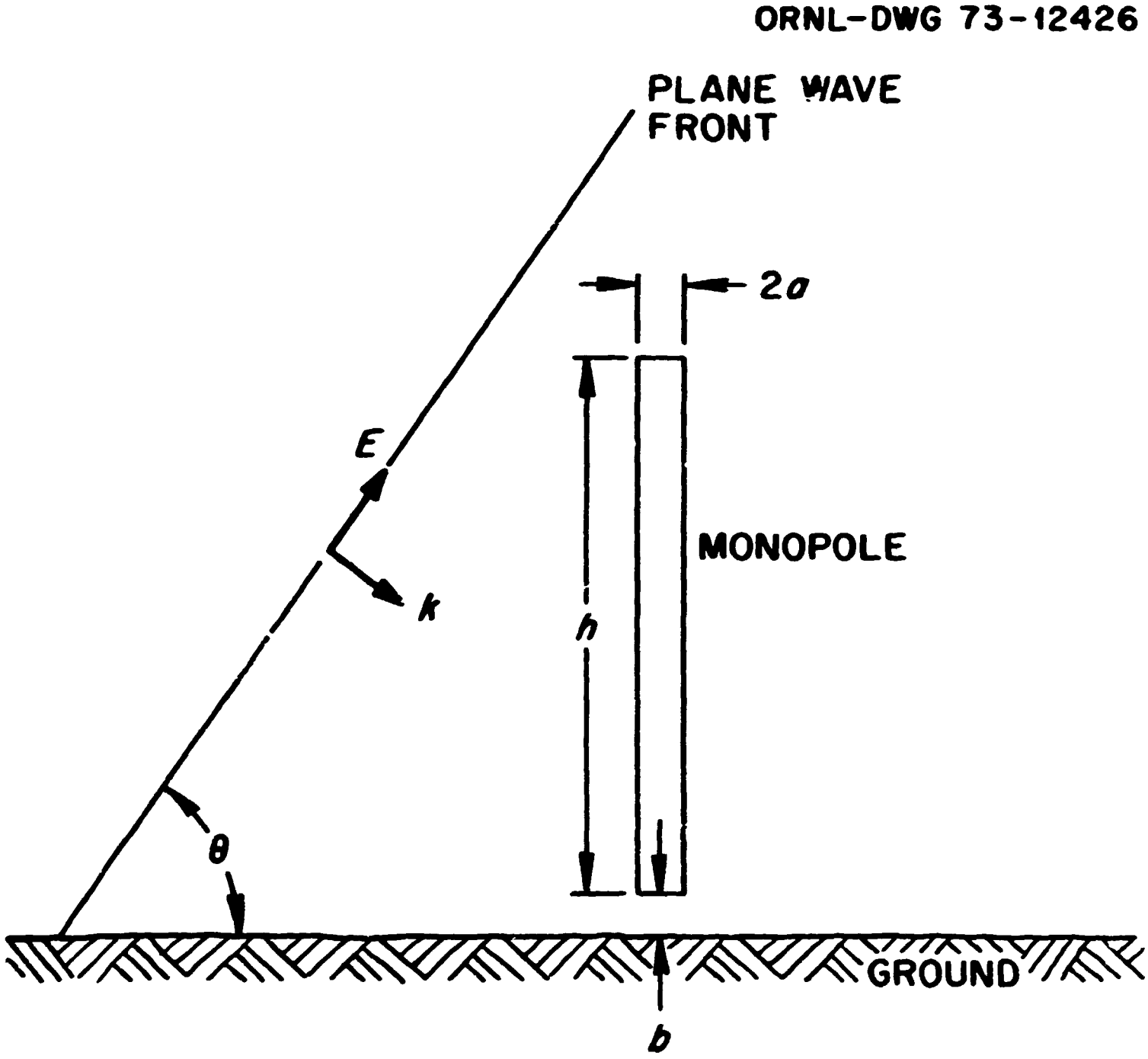

Fig. 1.1. Geometry of EMP-Antenna Interaction.

prone to many numerical difficulties. We have obtained good results from this model by careful selection of frequency points using the results from the other models.

For the applications we have considered a monopole approximately 360 meters tall and 0.8 meters in radius.* A top loading array has been included, albeit somewhat empirically. The matching network, inductive and resistive, resonates with the antenna at 34.5 kHz. Two representative EMP fields were considered; each of these was taken at two different angles of incidence. The response functions chosen were the short circuit current and the voltage across the load.

1.2 Electromagnetic Environment

References exist which describe EMP from high altitude nuclear detonations.[8,9] For our purposes we idealize the EMP to a plane wave with the propagation vector in an arbitrary direction. For simplicity the electric field is taken to lie in the plane formed by the antenna and the propagation vector. This polarization results in a horizontal magnetic field. Figure 1.1 illustrates the geometry of the wave-antenna-ground system. The angle of incidence is θ; broadside incidence corresponds to 90°. For the examples, we have chosen θ to be 90° and 30°.

The time dependence of the electric field is idealized to a double exponential

$$E(t) = E_o\left(e^{-\alpha t} - e^{-\beta t}\right) \quad . \tag{1.1}$$

Two different sets of parameters have been chosen: a short pulse with E_o, α, and β given by

$$\begin{aligned} E_c &= 1.61 \times 10^5 \text{ V/m} \\ \alpha &= 5.00 \times 10^7 \text{ sec}^{-1} \\ \beta &= 1.76 \times 10^8 \text{ sec}^{-1} \end{aligned} \tag{1.2}$$

---

*The term "monopole" is used in this paper to describe a half-dipole erected perpendicular to a ground plane.

and a long pulse with

$$E_0 = 4.20 \times 10^4 \text{ V/m}$$
$$\alpha = 4.00 \times 10^6 \text{ sec}^{-1} \qquad (1.3)$$
$$\beta = 4.76 \times 10^8 \text{ sec}^{-1} \quad .$$

These units correspond to time in seconds and electric field in volts/meter.

2. ANTENNA ANALYSIS

2.1 The Low-Frequency Radiator

The low-frequency (LF) vertical radiator generally consists of a vertical tower erected above a radial ground system. Since the physical height of the tower is normally less than one-eighth of the wavelength of the transmitting frequency, the LF vertical radiator is usually an electrically short antenna. The characteristics of an electrically short vertical radiator may be improved by adding a top-loading umbrella. The top loading tends to increase the antenna's effective height and decrease the voltage between the base of the tower and the ground system. The geometry of a typical LF vertical radiator is shown in Fig. 2.1.

When the LF transmitter antenna is viewed as a receiving device, its load is the transmitter and coupling circuitry. The antenna is normally connected to the coupling circuit by a short wire-above-ground transmission line. The inductive reactance of the coupling circuit and the transmitter is adjusted to cancel the antenna's capacitive reactance at the transmitter carrier frequency. Also, the resistance of the coupling circuit and transmitter is designed to match the radiation resistance of the vertical radiator for maximum power transfer. The value of that resistance is normally on the order of 1 ohm. A typical LF transmitter output circuit is shown in Fig. 2.2a. Z_t is the impedance of the transmitter and the remaining coupling circuitry.

When an antenna is considered as a receiving device it is useful to employ a Thevenin or a Norton equivalent circuit. The Thevenin and Norton equivalent circuits are shown in Figs. 2.2b and 2.2c, respectively. The equivalent circuit parameters are defined below:

V - voltage across the load

I - current through the load

Z_L - load impedance

Y_L - load admittance

ORNL-DWG 73-9567

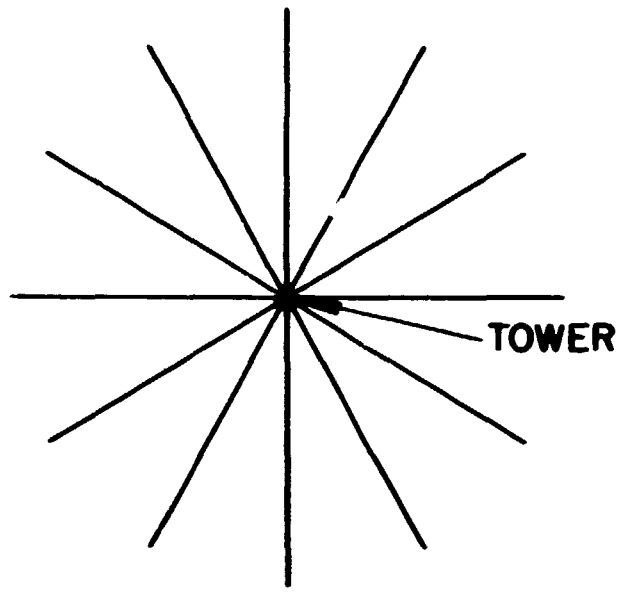

(*a*) TOP VIEW - VERTICAL RADIATOR WITH TOP-LOADING UMBRELLA.

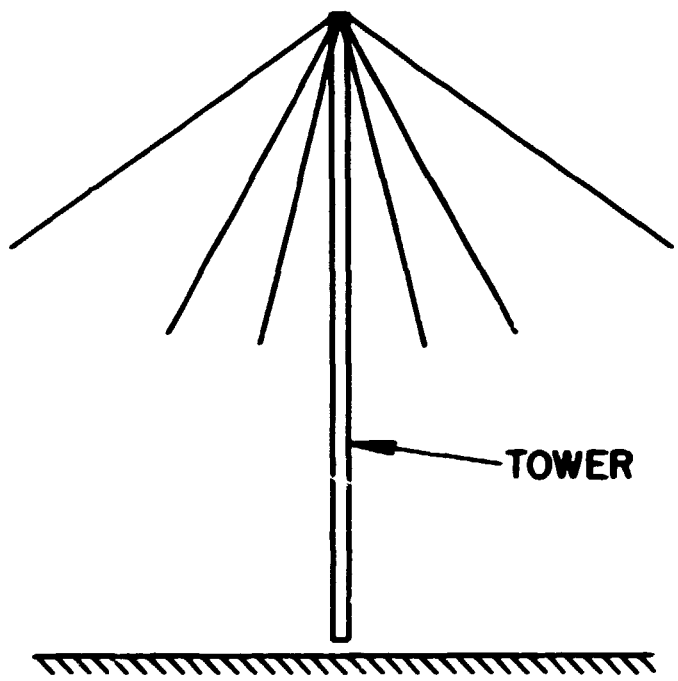

(*b*) SIDE VIEW - VERTICAL RADIATOR WITH TOP-LOADING UMBRELLA.

Fig. 2.1. Typical LF Vertical Radiator.

ORNL-DWG 73-9568

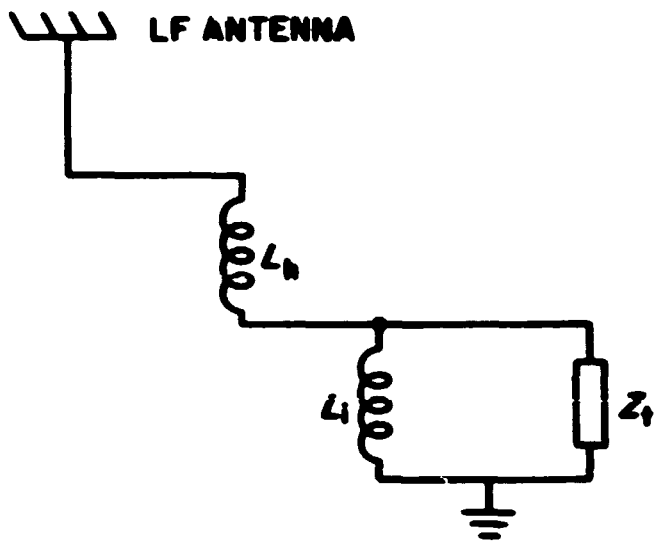

(a) LF ANTENNA AND LOAD

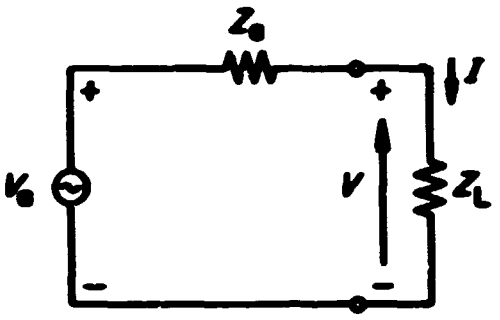

(b) THEVENIN EQUIVALENT CIRCUIT

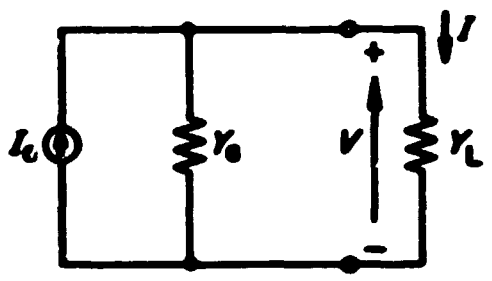

(c) NORTON EQUIVALENT CIRCUIT

Fig. 2.2. Equivalent Circuits for Determining the LF Antenna Response.

Z_a - impedance of the antenna

Y_a - admittance of the antenna

V_a - equivalent voltage source of the antenna and the electromagnetic environment

I_a - equivalent current source of the antenna and the electromagnetic environment.

Once the equivalent circuit parameters have been determined, the load response can be calculated by circuit theory. The following circuit relationships apply:

$$V = \frac{V_a Z_L}{Z_a + Z_L} = \frac{I_a}{Y_a + Y_L} \tag{2.1}$$

$$I = \frac{I_a Y_L}{Y_a + Y_L} = \frac{V_a}{Z_a + Z_L} \tag{2.2}$$

$$I_a = V_a Y_a \quad . \tag{2.3}$$

Also, from Fig. 2.2a the load impedance is given by

$$Z_L(\omega) = j\omega L_h + \frac{j\omega L_i Z_t}{Z_t + j\omega L_i} \quad . \tag{2.4}$$

For the purpose of calculating the equivalent circuit parameters, a thin cylindrical antenna can be used. A thin cylindrical antenna with a noncircular cross section such as a solid tower behaves like a circular cylindrical antenna with an equivalent radius. For frequencies of interest, the tower behaves like a solid structure. The equivalent radius of a tower with an equilateral triangular cross section is[10]

$$a_e = .42a_c \tag{2.5}$$

where a_c is the radius of the circle which circumscribes the equilateral triangle.

2.2 Early Time Model

The vertical tower radiator can be idealized by an early time model consisting of semi-infinitely long, perfectly conducting, circular cylinder erected perpendicular to a perfectly conducting ground plane as shown in Fig. 2.3. The time domain solution of the infinite antenna response is the same as that of the finite antenna for early times, i.e., times before the reflections from the top of the finite structure have effect.

The Norton equivalent current source for a semi-infinite, perfectly conducting, cylindrical structure of radius "a" erected above a perfectly conducting ground plane is twice that of an infinite cylindrical antenna and is given by[1]

$$I_a(s) = \frac{4\pi cE(s)}{\zeta \sin\theta\, sK_0(as\sin\theta/c)} \tag{2.6}$$

where s is the Laplace transform variable, $E(s)$ is the Laplace transform of the incident wave time history, ζ is the free space wave impedance approximately equal to 120π ohms, c is the free space speed of light and θ is the angle of incidence measured from the axis of the antenna.

The admittance of the semi-infinite cylindrical antenna separated from the ground plane by a gap distance "b" can be derived from that of an infinite cylindrical antenna as[1]

$$Y_a(s) = \frac{2as}{c\psi\zeta}\int_{-\infty}^{\infty} \frac{\sin(\psi\xi)K_1(u)}{\xi u K_0(u)}\, d\xi \tag{2.7}$$

where

$$u = \sqrt{\xi^2 + (as/c)^2} \tag{2.8}$$

and

$$\psi = b/a \quad . \tag{2.9}$$

$K_i(u)$ is the modified Bessel function of the second kind and order i.

ORNL-DWG 73-9569

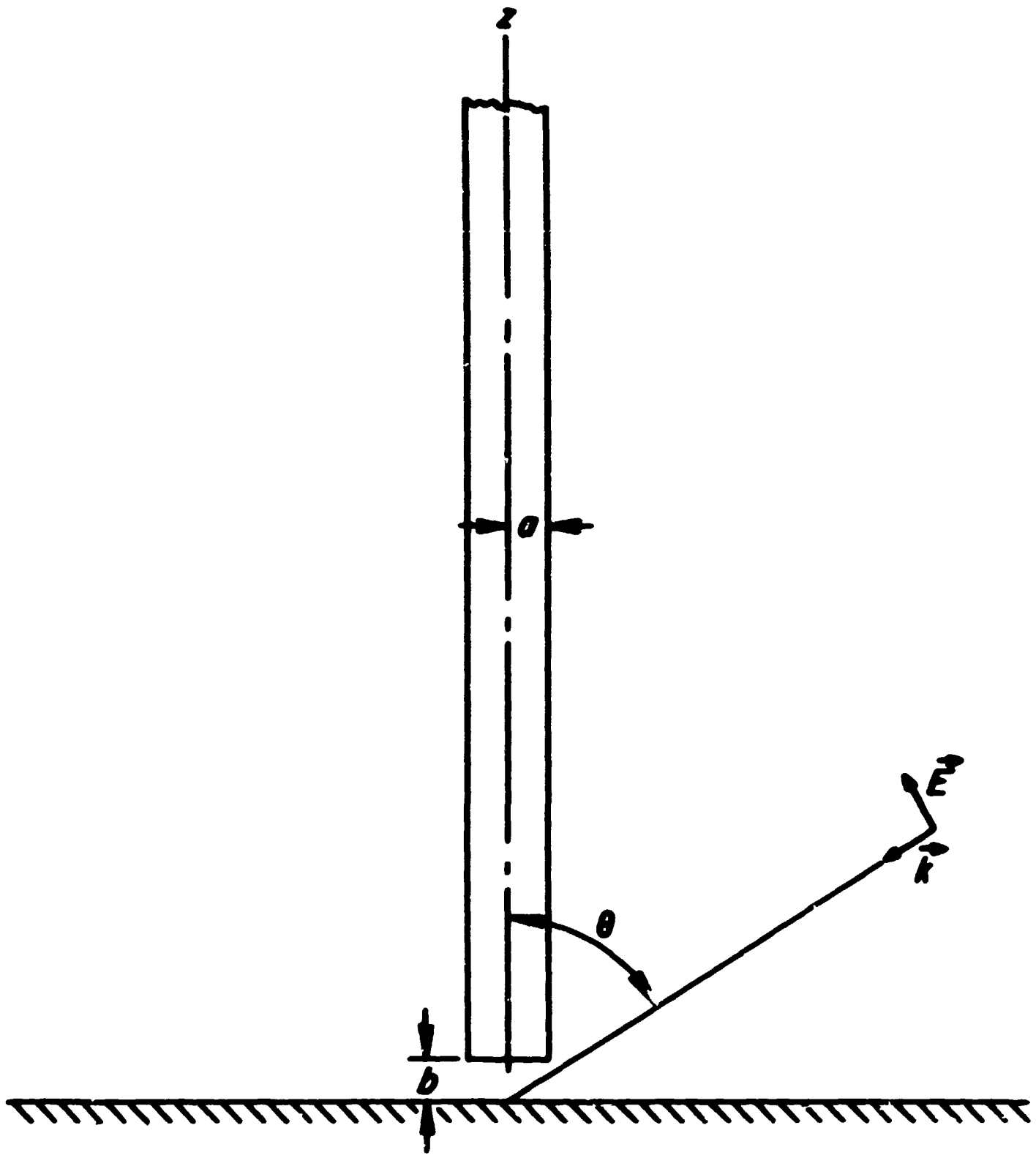

Fig. 2.3. Semi-Infinite Cylindrical Antenna and the Incident Plane Wave.

A simple early time asymptotic form of the voltage response across an inductive load can be derived for a double exponential incident wave using Equations (2.1), (2.6), and (2.7):[1]

$$V(t) \sim \frac{8\psi_a E_0 (\beta-\alpha)t}{3\pi} \sqrt{\frac{2ct}{a \sin\theta}} \qquad (2.10)$$

where the time history of the incident wave is given by

$$E(t) = E_0\left(e^{-\alpha t} - e^{-\beta t}\right) \qquad (2.11)$$

and time t equal zero corresponds to the time that the incident wave reaches the equivalent driving point of the antenna. From Eq. (2.10), it is evident that the first term in the asymptotic expansion of the voltage response across an inductive load is not a function of the inductance. This is a reasonable result since at early times (high frequencies) the inductance has a near infinite impedance and the first term of the solution for the load voltage is equal to that of the open circuit voltage response.

2.3 Moderate and Late Time Models

For moderate and late time, the length of the structure and the top-loading umbrella have important effects on the response of the vertical radiator. The finite length produces end reflections in the time domain. The top-loading umbrella adds more resonances corresponding to the umbrella-vertical antenna-ground system. It affects the quasi-static (low frequency) antenna parameters by increasing both the static antenna capacitance and the effective length.

The finite length thin monopole (or dipole) has been studied extensively. The methods we use, the singularity expansion method and the theories of King, Wu and Shen, are outlined in Sections 2.4 and 2.5. However, a rigorous treatment of the umbrella is not extant for the wide frequency range required. An empirical approach is used here, matching the quasi-static behavior of the radiator. In this approximation the low

frequency admittance of the antenna is modified to agree with the quasi-static capacitance of the monopole plus umbrella, while a fictitious height h is chosen equal to twice the low-frequency limit of the effective height of the antenna.

The quasi-static response of the LF vertical radiator is a first order approximation for the moderate and late time response of the structure. This can be inferred from the time domain solution by the singularity expansion method (SEM).[7] For moderate and late times, only the singularities near the origin in the complex frequency plane contribute appreciably to the solution. Thus, it is the low-frequency singularities that are important for the moderate and late time response.

Because the modifications due to the umbrella differ slightly in the two theories used for moderate and late time behavior, they are discussed separately in the next two sections.

2.4 Application of the Singularity Expansion Method

A new technique to calculate the dominant electric cylindrical dipole and monopole antenna responses to a transient electromagnetic plane wave pulse has been described in a previous report.[7] Basically, it involves applying the singularity expansion method formulated by Baum.[6] This method expands the frequency domain solution in terms of its singularities. The time domain solution is the inverse Laplace transform of each term in the frequency domain singularity expansion.

The Norton equivalent circuit parameters for a cylindrical monopole antenna can be expressed in terms of their singularities as[7]

$$I_a(s) = 8hsE(s)\sum_{m=1}^{M} \frac{A_m(s+\gamma_m) + B_m\omega_m}{(s+\gamma_m)^2 + \omega_m^2} \tag{2.12}$$

and

$$Y_a(s) = 2\sum_{m=1}^{M} \frac{sK_m\omega_m}{(s+\gamma_m)^2 + \omega_m^2} \quad . \tag{2.13}$$

The constants γ_m and ω_m are the natural damping constants and the natural resonant frequencies respectively and are functions of the antenna parameters only. The constants A_m and B_m determine the amplitude of the current and are functions of both the antenna parameters and the angle of incidence of the transient electromagnetic pulse. E(s) is the Laplace transform of the incident field time history and h is the physical height of the antenna. The constants K_m determine the amplitude of the admittance and the constant M is the number of singularities considered in the solution. The values of the constant quantities defined above are listed in Ref. 7 for broadside incidence and a wide range of antenna length-to-radius ratios. They have not yet been considered by Barnes for other angles.

The method employed in Ref. 7 to derive the singularity expansion quantities of the monopole admittance is accurate for frequencies equal to or less than the third resonance of the antenna. With M = 3 an accurate solution can be obtained for late times, i.e., $t \geq 6h/c$. If five singularities are used, the solution is within a few percent of the exact solution for times $t > h/c$. However, for $t \leq h/c$ large errors could result due to the inaccuracy of the admittance function.

The modifications necessary to account for the top-loading umbrella are indicated in Fig. 2.4. The actual height is replaced by a fictitious height h, equal to twice the low frequency limit of the effective height of the antenna. The equivalent admittance network of the quasi-static model is shown in Fig. 2.4b. The admittance of the cylindrical monopole has been modified by the addition of C_t, the capacitance due to the top-loading umbrella, to that part of the network consisting of R_1, L_1 and C_1 which is associated with the first resonance of the antenna. Y_{a-1} is the admittance of the remaining part of the equivalent antenna admittance network. The total antenna admittance can be written as

$$Y_a = Y_{a-1} + \frac{s(C_1 + C_t)}{1 + s^2 L_1 (C_1 + C_t) + sR_1(s)(C_1 + C_t)} \qquad (2.14)$$

and, of course, the antenna impedance is given by

ORNL-DWG 73-12142

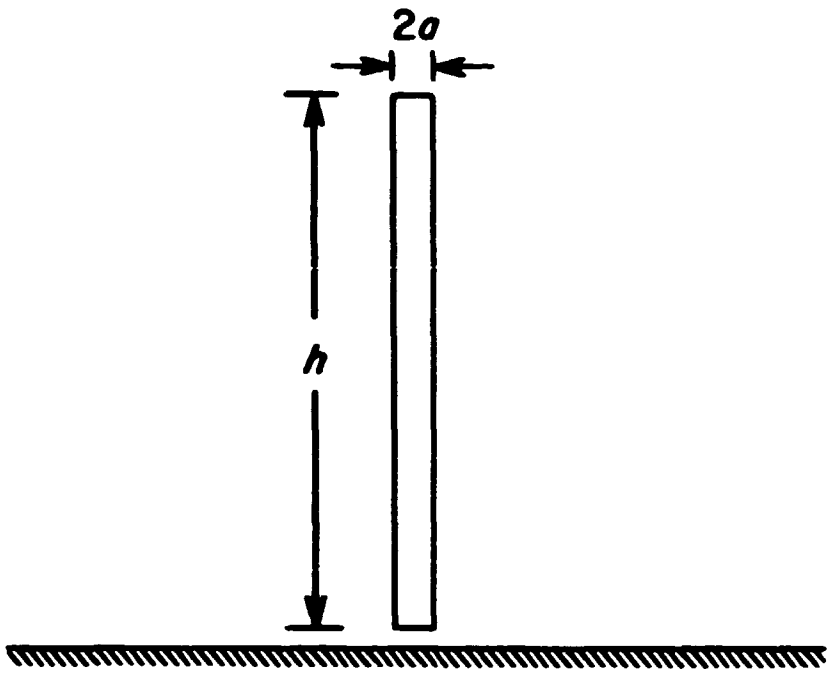

(a) PHYSICAL MODEL FOR CALCULATING THE EQUIVALENT NORTON CURRENT AND THEVENIN VOLTAGE SOURCES – A CYLINDRICAL MONOPOLE OF LENGTH h.

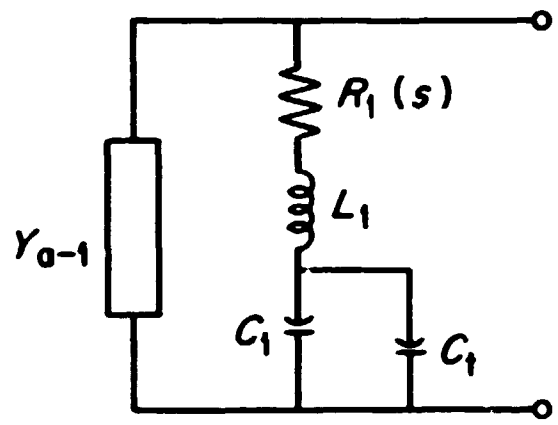

(b) EQUIVALENT ADMITTANCE NETWORK OF THE TOP-LOADED ANTENNA.

Fig. 2.4. Quasi-Static Model of the LF Vertical Radiator.

$$Z_a = Y_a^{-1} \tag{2.15}$$

For $t \geq 10\,h/c$, the solution for broadside incidence can be accurately characterized by only one singularity.[11] If only one singularity is used, the Norton circuit parameters are given by

$$I_a = 8hsE(s)\,\frac{[A(s+\gamma) + B\omega_1]}{(s+\gamma)^2 + \omega_1^2} \tag{2.16}$$

and

$$Y_a = \frac{2sK\omega_1}{(s+\gamma)^2 + \omega_1^2} \tag{2.17}$$

where the "1" subscripts have been dropped for A_1, B_1, K_1, and γ_1.

The current through an inductive load L due to the first singularity is

$$I = \frac{8hsE(s)\,[A(s+\gamma) + B\omega_1]}{(s+\gamma)^2 + \omega_1 + 2s^2K\omega_1L} \quad . \tag{2.18}$$

The value of K can be computed approximately from the antenna static capacitance C_0, which includes the top-loading capacitance, by

$$K = \frac{C_0(\gamma^2 + \omega_1^2)}{2\omega_1} \quad . \tag{2.19}$$

For the electrically short antenna

$$\omega_1^2LC_0 \gg 1 \quad . \tag{2.20}$$

and we can also observe from Ref. 7 that for thin cylindrical antennas

$$B \gg A \tag{2.21}$$

and

$$\omega^2 >> \gamma^2 \quad . \tag{2.22}$$

Substituting Eqs. (2.19) and (2.20), (2.21) and (2.22) into Eq. (2.18) and performing the inverse Laplace transform gives an approximate late time current response to an exponentially decaying incident pulse

$$i(t) = 8hE_0 \frac{(\omega')^2}{\omega_1 \alpha} Be^{-\gamma' t} \cos \omega' t \tag{2.23}$$

where

$$\omega' = \frac{1}{\sqrt{LC_0}} \tag{2.24}$$

$$\gamma' = \frac{\gamma \omega'^2}{(\gamma^2 + \omega_1^2)} \tag{2.25}$$

and time history of the incident wave is

$$E(t) = E_0 e^{-\alpha t} \tag{2.26}$$

where $\alpha >> (\gamma' + \omega')$.

The late time voltage across the inductor is given approximately by

$$V = L \frac{di}{dt} \simeq \frac{-8hE_0 L(\omega')^3 Be^{-\gamma' t}}{\omega_1 \alpha} \sin \omega' t \quad . \tag{2.27}$$

2.5 The Classical Antenna Theories

The classical theories of the monopole stem from the work of King[2] on the electrically short antenna and the treatment by Wu[3] of the electrically long antenna, with later simplications.[4,5] The Thevenin equivalent of the antenna, shown in Fig. 2.1b, is determined by two functions of radian frequency ω ($j\omega = s$, the Laplace transform variable

used before): the antenna impedance $Z_a(\omega)$, and the effective height $h_e(\omega)$. $Z_a(\omega)$ is used directly in Thevenin equivalent, and $h_e(\omega)$ determines the voltage source $V_a(\omega)$ through the formula

$$V_a(\omega) = -2h_e(\omega)E_v(\omega) \quad . \tag{2.28}$$

Here $E_v(\omega)$ is the component of the free space incident electric field parallel to the antenna. Ground reflection (equivalently, the antenna image) accounts for the factor of two in the formula.

Different functional forms for Z_a and h_e are used for electrically short and electrically long antennas. With k defined by $k = \omega/c$, where c is the speed of light, the dividing line is $kh = 1$. For $kh < 1$ the antenna is electrically short, and the relevant formulas are[12]

$$Z_a(\omega) = -\frac{j\zeta\Psi_{d\ell}\cos kh}{4\pi}\left[\sin kh + T(kh)\,(1 - \cos kh)\right]^{-1} \tag{2.29}$$

$$h_e(\omega) = \frac{\cos\,(kh\cos\theta) - \cos kh}{k\sin\theta\ \sin kh} \tag{2.30}$$

with

ζ = free space impedance $\simeq 120\pi$

ω = radian frequency

$\Psi_{d\ell} = 2\ell n\,\frac{h}{a} - 2$

h = antenna height

a = antenna radius

$$T(kh) = \frac{\left(2\ell n\,2 - \frac{2}{3}\right)kh - j\frac{2}{3}(kh)^2}{2\ell n\,(2h/a) - 3} \quad .$$

For $kh > 1$ the antenna is electrically long and the formulas of Wu[3] are

used. Since Wu assumed a time dependence $\exp(-i\omega t)$, instead of $\exp(j\omega t)$, the complex conjugate (*) of some of his quantities is required for agreement with the rest of this report. Z_a and h_e are

$$Z_a(\omega) = \left[\frac{2jk}{\omega\mu_o}(S + CU)\right]^{*\,-1} \tag{2.31}$$

$$h_e(\omega) = -\frac{j\pi Z_a(\omega)}{k\zeta}\,\frac{\sin\theta}{\Omega_1 - \ell n \sin\theta}\cdot$$

$$\cdot\left\{C^*\left[\frac{\sin\,[kh(1-\cos\theta)]}{1-\cos\theta} + \frac{\sin\,[kh(1+\cos\theta)]}{1+\cos\theta}\right]\right. \tag{2.32}$$

$$\left. + \frac{1}{2}\left[\frac{1-\cos\,[kh(1-\cos\theta)]}{1-\cos\theta} + \frac{1-\cos\,[kh(1+\cos\theta)]}{1+\cos\theta}\right]\right\}$$

Here

$$C = -\frac{1}{2}\,\frac{(2T-T')\sin kh - (2S-S')\cos kh}{T'\cos kh + S'\sin kh}$$

$$U = -j(A_2 - A_3)$$

$$\gamma \approx 0.57722$$

$$\gamma' \approx 1.6449$$

$$\Omega_0 = \ell n\,(2/ka) - \gamma$$

$$\Omega_0' = \Omega_0 - \ell n\,2$$

$$\Omega_1 = \Omega_0 + j\pi/2$$

$$\Omega_2 = 2\,\Omega_0' + \ell n\,2kh + \gamma - j\pi/2$$

$$\Omega_2' = \Omega_2 + \ell n\,2$$

$$\Omega_3 = \Omega_2 + j2\pi$$

$$\Omega_3' = \Omega_2' + j2\pi$$

$$A_1 = \ln\left[1 + \frac{j\pi}{\Omega_0'}\right] + \frac{\pi^2}{12}\left[\frac{1}{(\Omega_3' - \ln 2)^2} - \frac{1}{(\Omega_0' - \ln 2 + j\pi)^2}\right]$$

$$A_2 = \ln(\Omega_3/\Omega_2) + \frac{1}{2}\gamma'(\Omega_3^{-2} - \Omega_3^{-2})$$

$$A_2' = \ln(\Omega_3'/\Omega_2') + \frac{1}{2}\gamma'(\Omega_2'^{-2} - \Omega_3'^{-2})$$

$$A_3 = \frac{-j}{2kh} e^{2jkh}(\Omega_2^{-1} - \Omega_3^{-1})$$

$$A_3' = \frac{-j}{4kh} e^{4jkh}(\Omega_2'^{-1} - \Omega_3'^{-1})$$

$$S = \frac{1}{2}(-A_1 + A_2 + A_3)$$

$$S' = \frac{j}{2}(-A_1 + A_2' + A_3')$$

$$T = \frac{j}{2}(-A_1 - A_2 + A_3)$$

$$T' = \frac{j}{2}(-A_1 - A_2' + A_3') \quad .$$

The formulas of Wu are quite complicated. More recently, two papers by King, Wu and Shen[4,5] developed a simple theory of the long transmitting and receiving linear antenna which uses much more intuitive techniques than the Wiener-Hopf method of Wu. The resulting formulas for Z_a and h_e are correspondingly simpler. A further advantage of this theory is that its starting point is the current induced by a plane wave in an infinite circular cylinder, our Eq. (2.6). In undertaking the present study we were particularly interested in the variation of antenna response with angle of incidence θ. Equation (2.6) shows this to be approximately as $\sin^{-1}\theta$. (The apparent singularity at $\theta = 0$ is removed when finite antenna conductivity is included. The infinite conductivity model gives

approximately the same results as the finite conductivity model with reasonable conductivity values until θ is equal to or less than some small angle.) This fact means that the standard treatment, broadside incidence, produces the least current in an infinite wire. As we are in general interested in worst case response, it is important to consider angles of incidence other than broadside when studying long antennas such as the LF monopole. The formulas of Ref. 5 allow easier understanding of the variation in effective height with θ than do those of Wu.

This simple theory leads to computed values of $Z_a(\omega)$ and $h_e(\omega)$ which are virtually identical to those of Wu. The formulas are

$$Z_a^* = \frac{1}{2} I_0^{-1} \tag{2.33}$$

$$h_e^* = \frac{\pi I_{NL}}{k \sin\theta \, I_\infty(0)} \tag{2.34}$$

with

$$I_0 = I_\infty(0) + 2C_d I_\infty(h)$$

$$I_\infty(z) = \frac{j e^{jkz}}{\zeta} \ln\left[1 - \frac{2\pi j}{2C_\omega + \ln(kz + \sqrt{(kz)^2 + e^{-2\gamma}}) + \gamma + j\,3\pi/2}\right]$$

$$C_\omega = -\ln ka - \gamma$$

$$\gamma \approx 0.5772$$

$$\zeta \approx 120\pi$$

$$C_d = -RI_\infty(h)/[1 + RI_\infty(2h)]$$

$$I_{NL} = I_{s\infty}(0) + \left(C_{s1} + C_{s2}\right) I_{\infty}(h)$$

$$I_{s\infty}(z) = \frac{j \exp\ (jkz \cos\ \theta)}{\zeta \sin\ \theta \{C_{\infty} - \log\ [(\sin\ \theta)/2] + j\pi/2\}}$$

$$C_{s1} = \frac{RR_s(\pi-\theta)\, I_{s\infty}(h)\, I_{\infty}(2h) - I_{s\infty}(-h)\, R_s(\theta)}{1 - R^2 I_{\infty}^2(2h)}$$

$$C_{s2} = \frac{RR_s(\theta)\, I_{s\infty}(-h)\, I_{\infty}(2h) - I_{s\infty}(h)\, R_s(\pi-\theta)}{1 - R^2 I_{\infty}^2(2h)}$$

$$R = \frac{\zeta}{2\pi}\left(2C_{\infty} + j\pi\right)$$

$$R_s(\theta) = R - \frac{\zeta}{2\pi} \log\ [(1 - \cos\ \theta)/2] \quad .$$

All of the formulas given above are for a simple monopole above an infinitely conducting ground. The actual LF antenna uses a top-loading umbrella which affects both Z_a and h_e. A rigorous theory of this structure would be quite difficult to derive. Empirically it can be added to the classical theory in a manner very similar to that used in the singularity expansion method of Section 2.4. The change in effective height is simulated by a change in the real height h so that $h = 2h_e(0)$. The change in Z_a cannot be made exactly as in Section 2.4, because the values of L_1 and C_1 associated with the first antenna resonance are not readily obtainable from the classical theories. Instead the umbrella is treated quasi-statically as a LC resonant structure in parallel with the antenna reactance but in series with the antenna resistance. That is, Z_a is separated into real and imaginary parts:

$$Z_a(\omega) = R_a(\omega) + jX_a(\omega) \tag{2.35}$$

and the reactance of the umbrella is denoted by X_t:

$$X_t(\omega) = -1/\omega C_t + \omega L_t \quad . \tag{2.36}$$

Then the modified impedance Z_a' is

$$Z_a' = R_a + j\frac{X_a X_t}{X_a + X_t} \quad . \tag{2.37}$$

C_t is the known static capacitance of the umbrella, and since the horizontal length of the umbrella is approximately the same as the antenna height, L_t is chosen so the umbrella resonates at the first antenna resonance:

$$L_t C_t = \frac{4h^2}{c^2\pi^2} \quad . \tag{2.38}$$

While this treatment of the umbrella is certainly not rigorous, it is correct in both the low frequency and high frequency limits and presumably mirrors the gross behavior of the monopole-umbrella system.

3. ANTENNA RESPONSE CALCULATIONS

3.1 Introduction

The short-circuit current and load voltage response of an example LF transmitting antenna system to the two double exponential EMP's of Eqs. (1.1)-(1.3) are considered in this section. A 1200-foot top-loaded vertical tower radiator with an effective radius of 0.75 m is modeled by a cylindrical monopole antenna. One effect of the top-loading umbrella is to increase the effective length of the antenna from about 366 m to 450 m. Also, the static antenna capacitance is increased from about 4 nf to 14 nf by the top-loading umbrella. Thus the additional capacitance due to the top-loading, C_t, is 10 nf.

The models and calculational techniques described in Section 2 have been employed to calculate the response curves presented here. Plots calculated by the different methods are presented on the same graph for comparison.

3.2 The Short-Circuit Current

The short-circuit current responses of the vertical radiator to the long and short incident plane wave pulses are shown in Figs. 3.1, 3.2 and 3.3 with θ as a parameter. In Figs. 3.1 and 3.2, the early time and early-to-moderate time responses are shown respectively. The solid curves have been calculated by the classical antenna method and the dashed curves have been calculated by the exact solution of a semi-infinite cylindrical antenna with $\Psi = 1.0$. (Ψ is defined in Eq. 2.9.) The relative error of each dashed curve is less than 0.1%. In Fig. 3.2, the dashed curves are plotted for only the time intervals during which they are valid for the 1200-foot top-loaded antenna.

The classical antenna method can introduce errors in the early time results due to the limited frequency range feasible and numerical Fourier inversion used in the calculations. The highest frequency considered was $\omega = 0.8 \times 10^8$, which corresponds to a resolution of $t \approx 12$ nsec. However, as can be seen from Figs. 3.1 and 3.2, there is

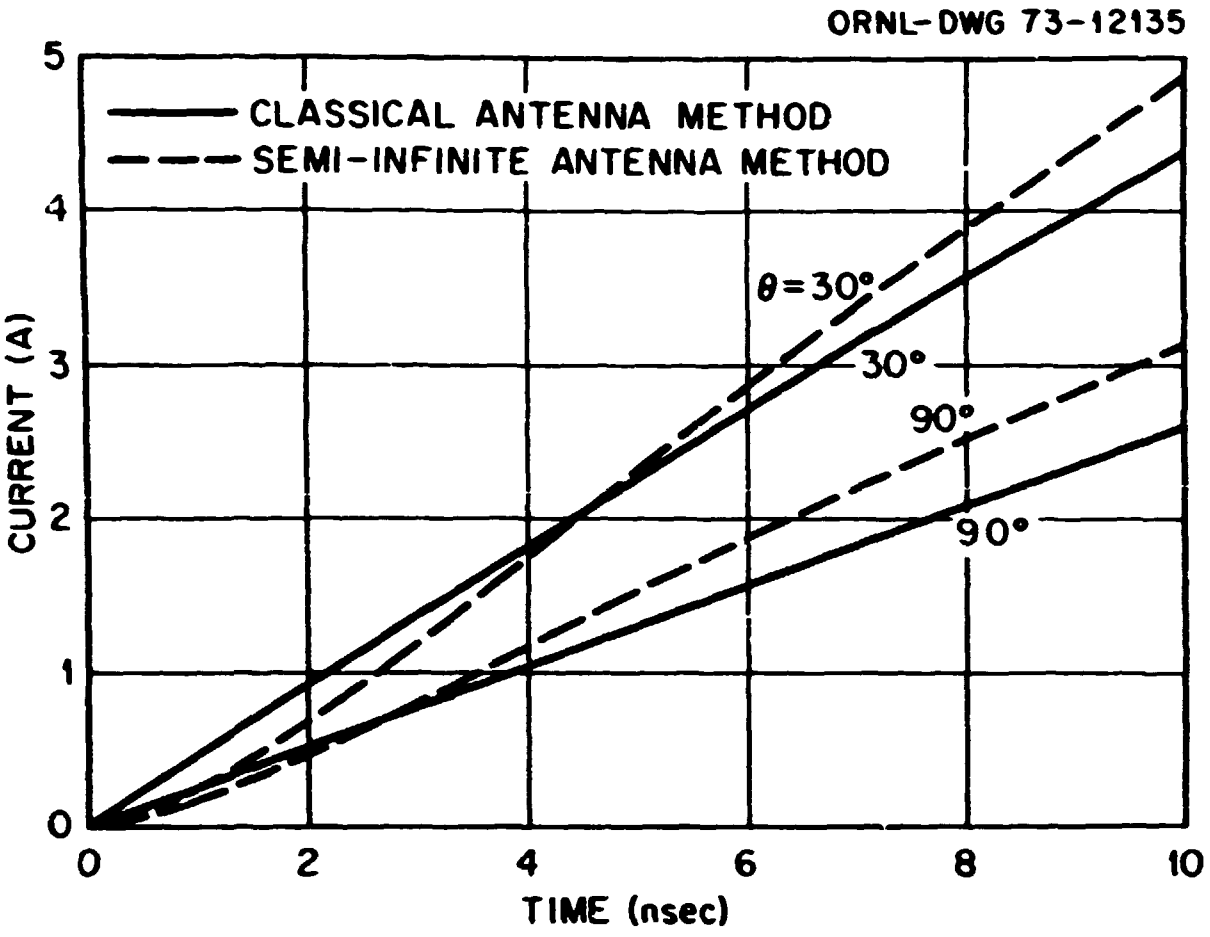

(a) RESPONSE TO THE SHORT PULSE

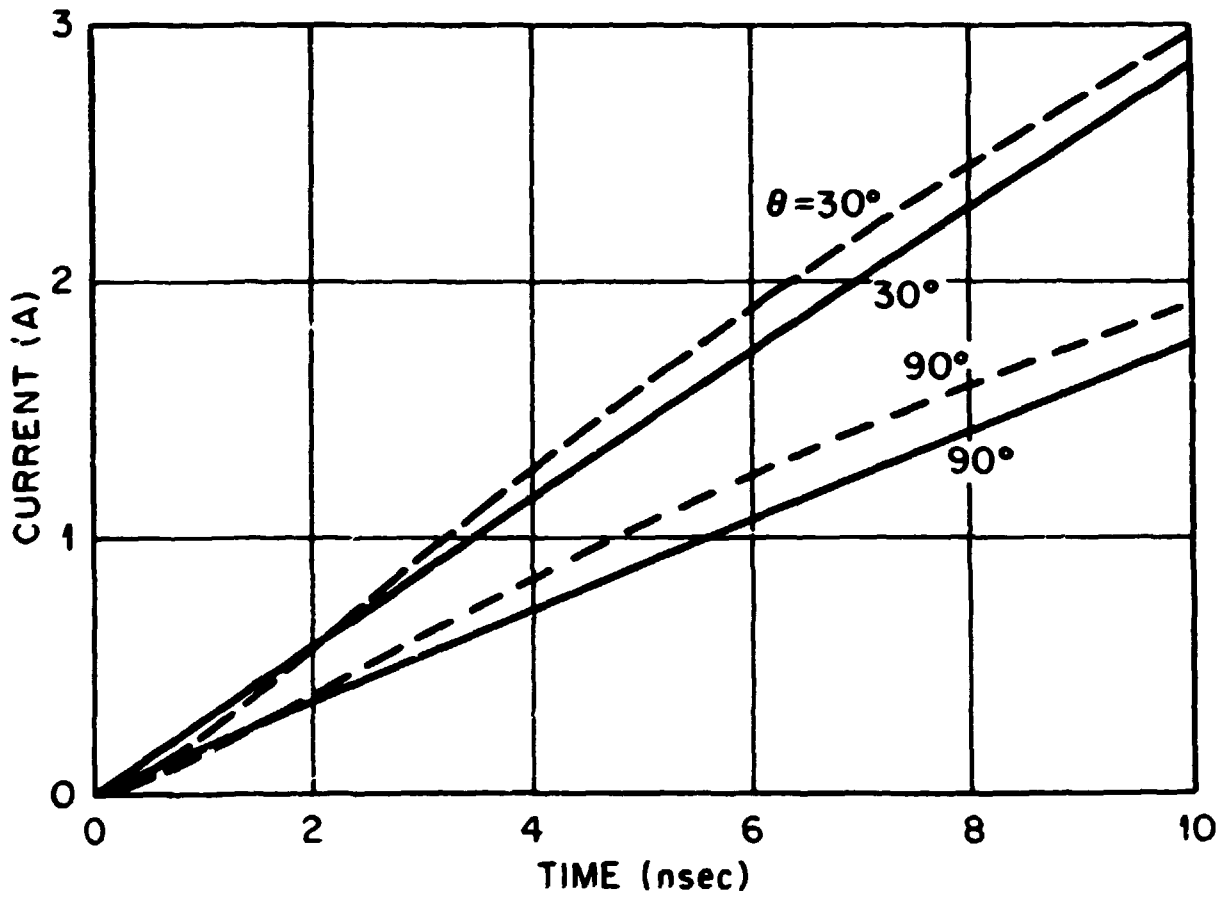

(b) RESPONSE TO THE LONG PULSE

Fig. 3.1. Early Time Short-Circuit Current Response.

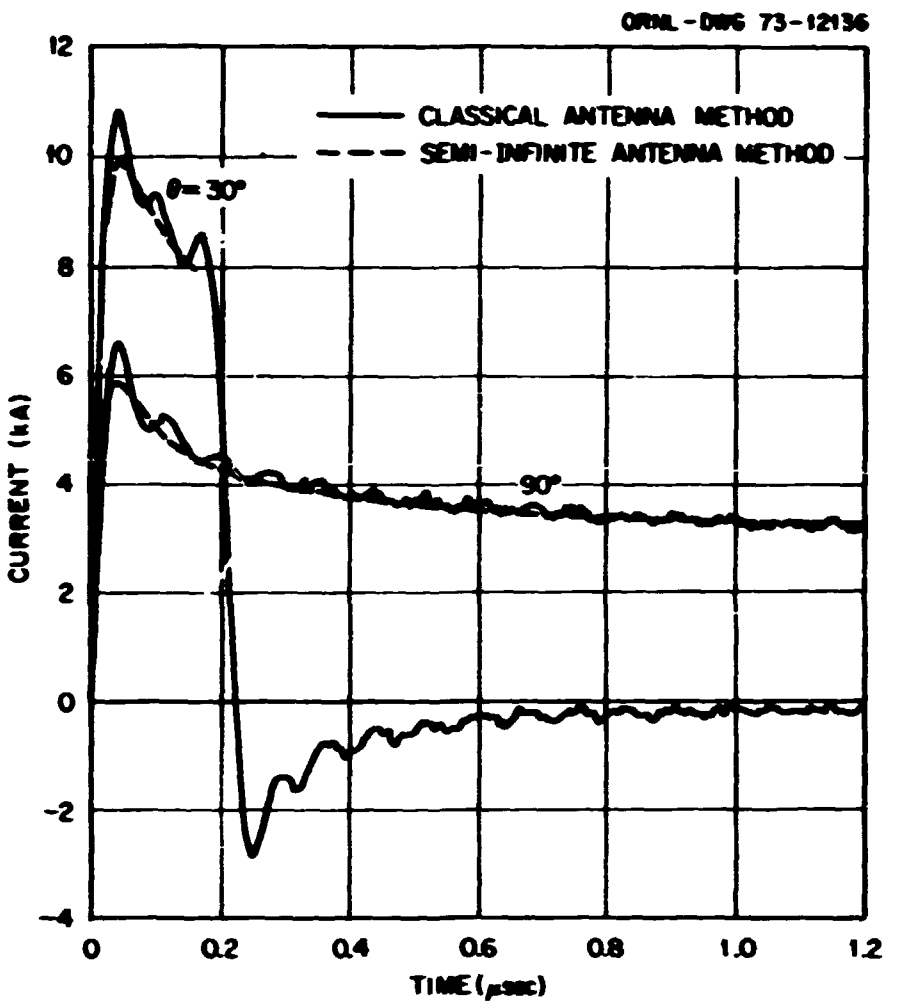

(a) RESPONSE TO THE SHORT PULSE

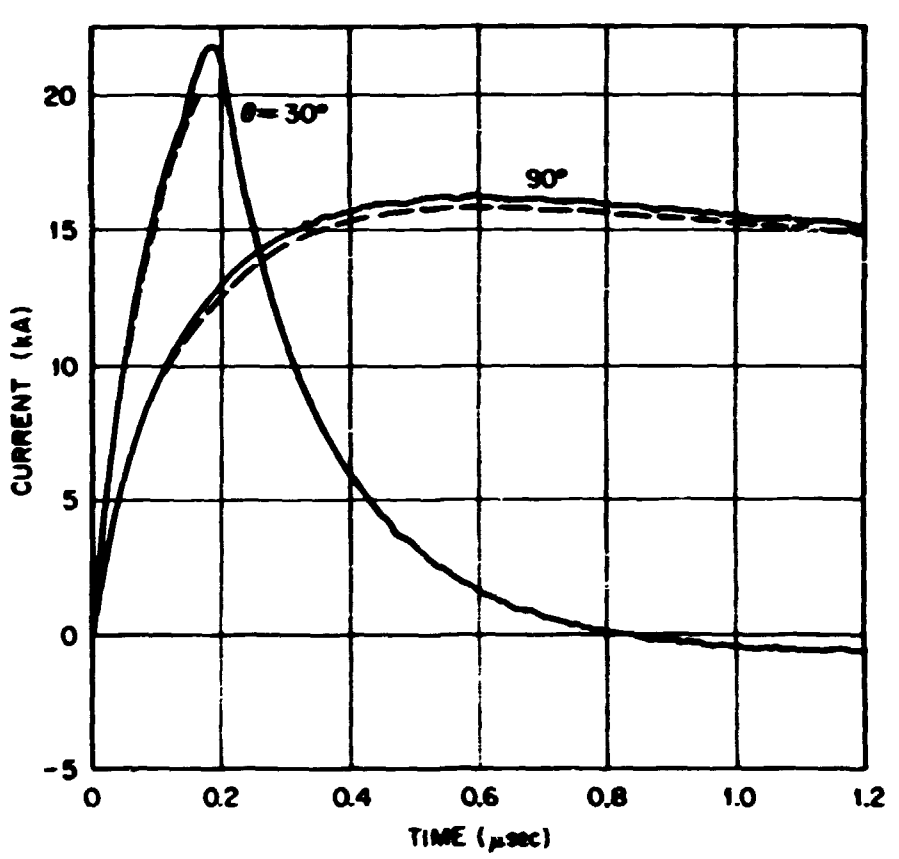

(b) RESPONSE TO THE LONG PULSE

Fig. 3.2. Early to Moderate Time Short-Circuit Current Response.

good agreement between the results calculated by the classical antenna method and the semi-infinite antenna method even for times less than 10 ns. Thus, the early time errors introduced by the classical antenna method are reasonably small.

In Fig. 3.3, the moderate time short-circuit current responses of the LF vertical radiator are shown. The dashed curves have been calculated for $\theta = 90°$ by the singularity expansion method employing five singularities. The solid curves have been computed by the classical antenna method with θ as a parameter. As can be observed from Fig. 3.3, there is good agreement between the two methods for times greater than 1.4 μsec. For earlier times, not enough singularities have been used to accurately compute the dashed curves.

3.3 The Load Voltage

The voltage responses across a typical LF load connected to the 1200-foot top-loaded vertical radiator are shown in Figs. 3.4 through 3.7. The load network shown in Fig. 2.2a with $L_h = 1.21$ mh, $L_i = 0.2$ mh and $Z_t = 1\Omega$ was used for the calculations. In all the figures the solid curves are the results as computed by the classical antenna method. The dashed curves are the results as calculated by the semi-infinite antenna method in Figs. 3.4 and 3.5 and by the singularity expansion method in Fig. 3.7. As can be seen from the plots, the solid and dashed curves are generally in good agreement.

In Fig. 3.6, only the classical antenna method was used to compute the load voltage responses. The singularity expansion method normally gives accurate results for moderate times; however, the formulation presently used by Barnes employs an approximation of the antenna admittance which gives inaccurate results for early-to-moderate times.

In Fig. 3.7, the late time load voltage responses are shown. The dashed curves were computed using only one singularity and are reasonably accurate for times greater than 20 μsec. As can be seen, there is good agreement between solid curves for $\theta = 90°$ and the dashed curves. Some numerical errors resulted from the Fourier inversion used by the

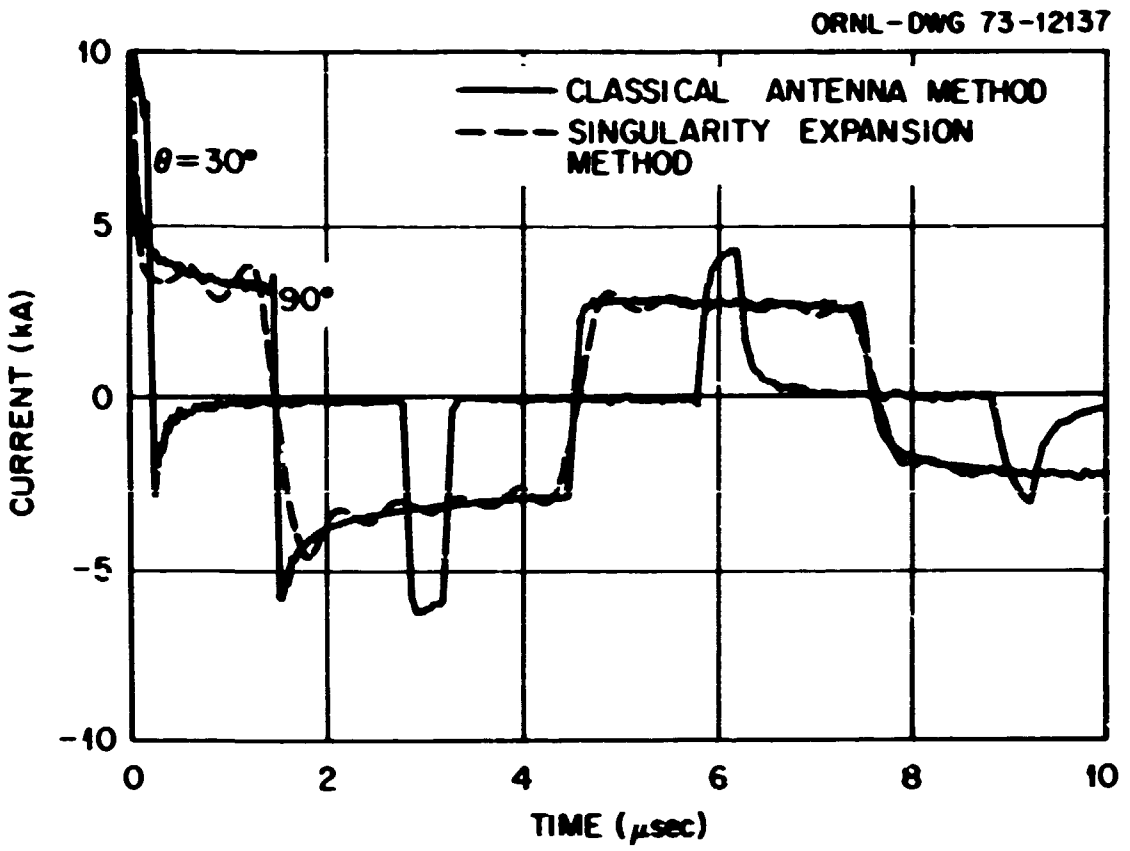

(a) RESPONSE TO THE SHORT PULSE

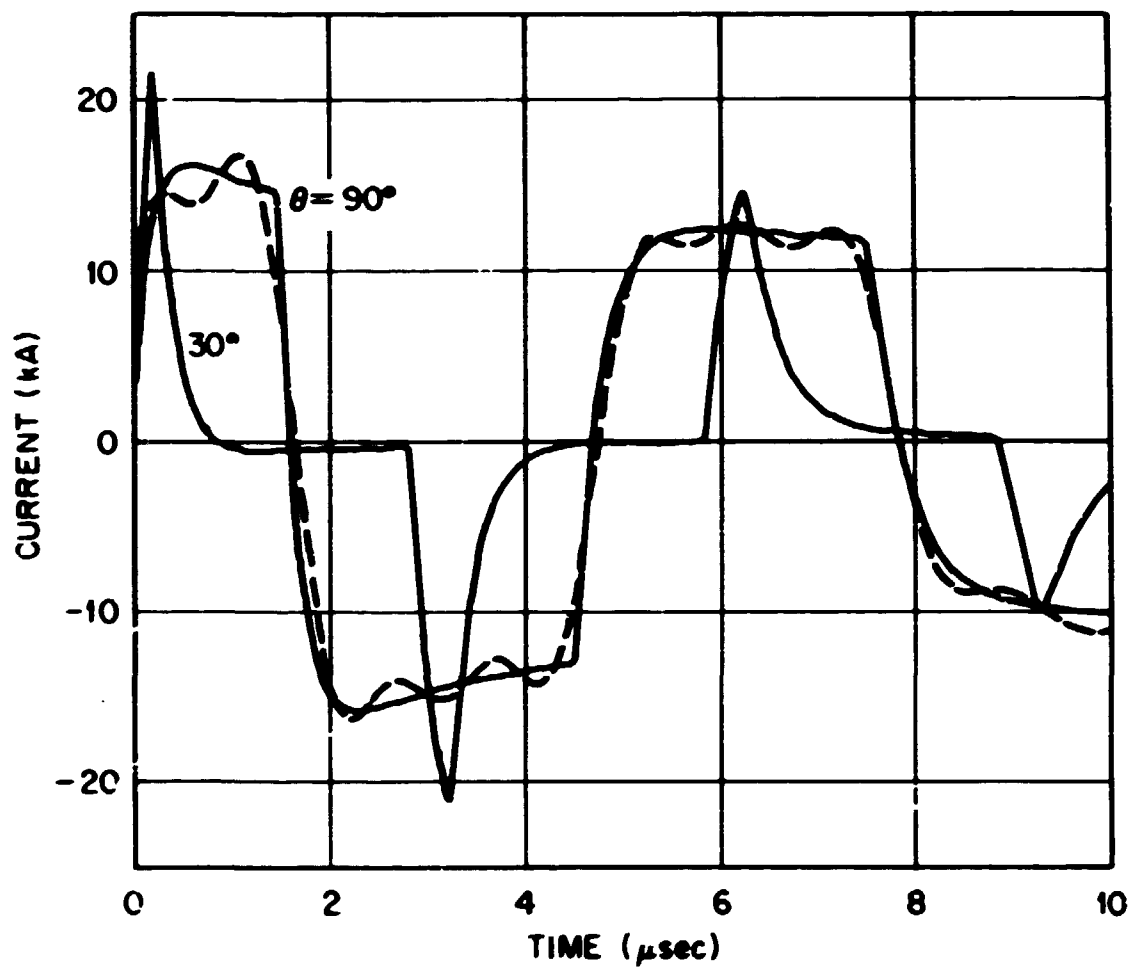

(b) RESPONSE TO THE LONG PULSE

Fig. 3.3. Moderate Time Short-Circuit Current Response.

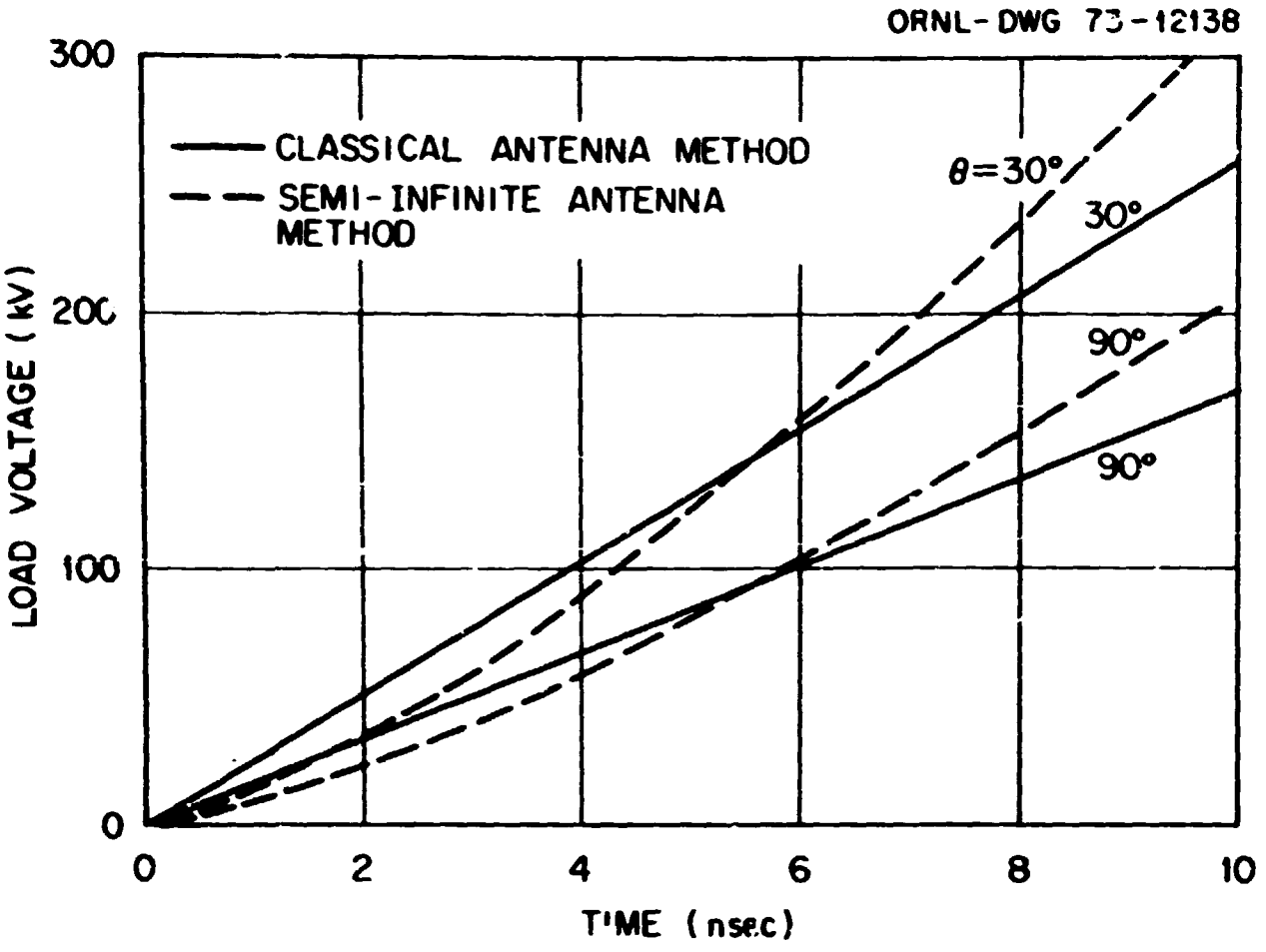

(a) RESPONSE TO THE SHORT PULSE

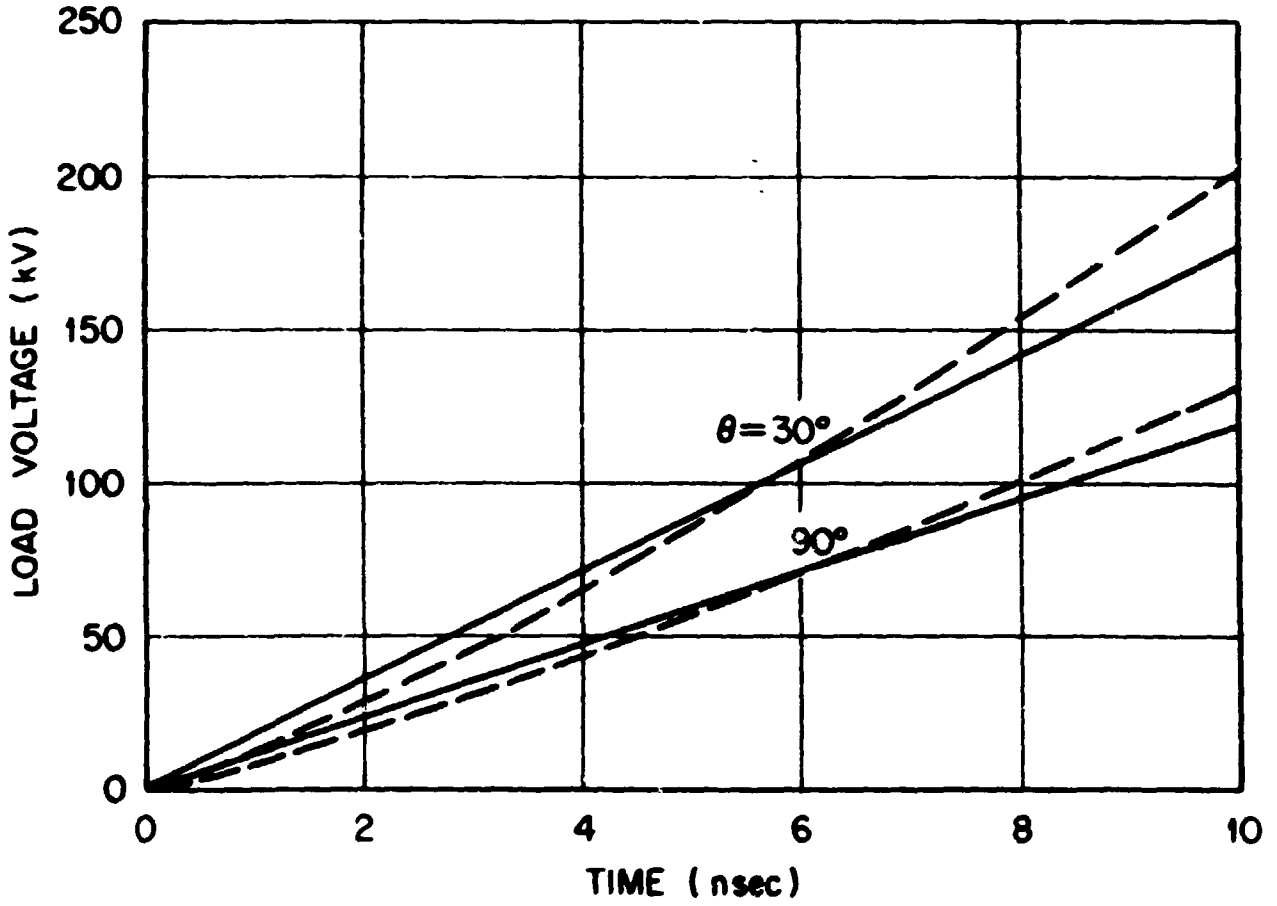

(b) RESPONSE TO THE LONG PULSE

Fig. 3.4. Early Time Load Voltage Response.

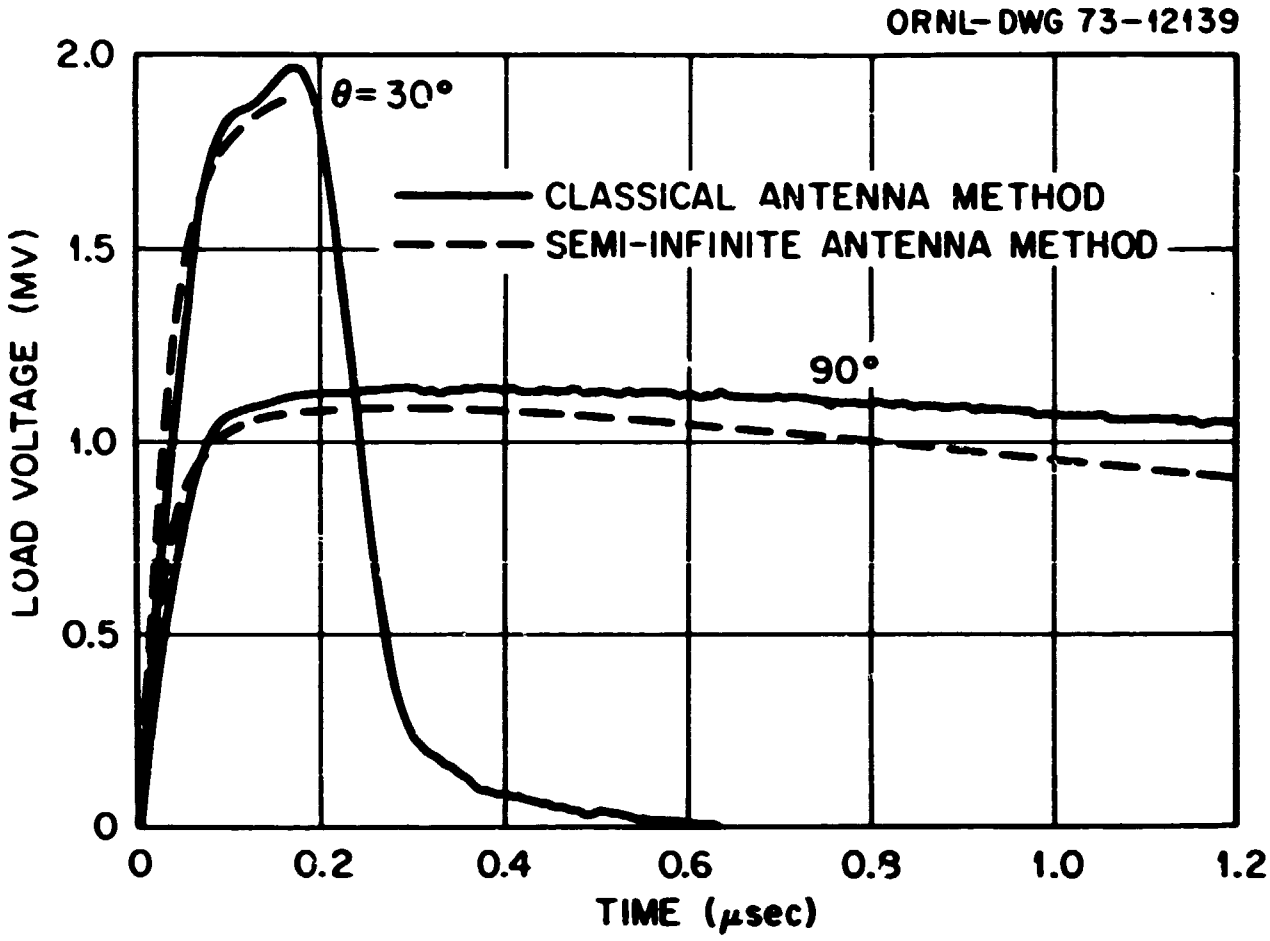

(*a*) RESPONSE TO THE SHORT PULSE

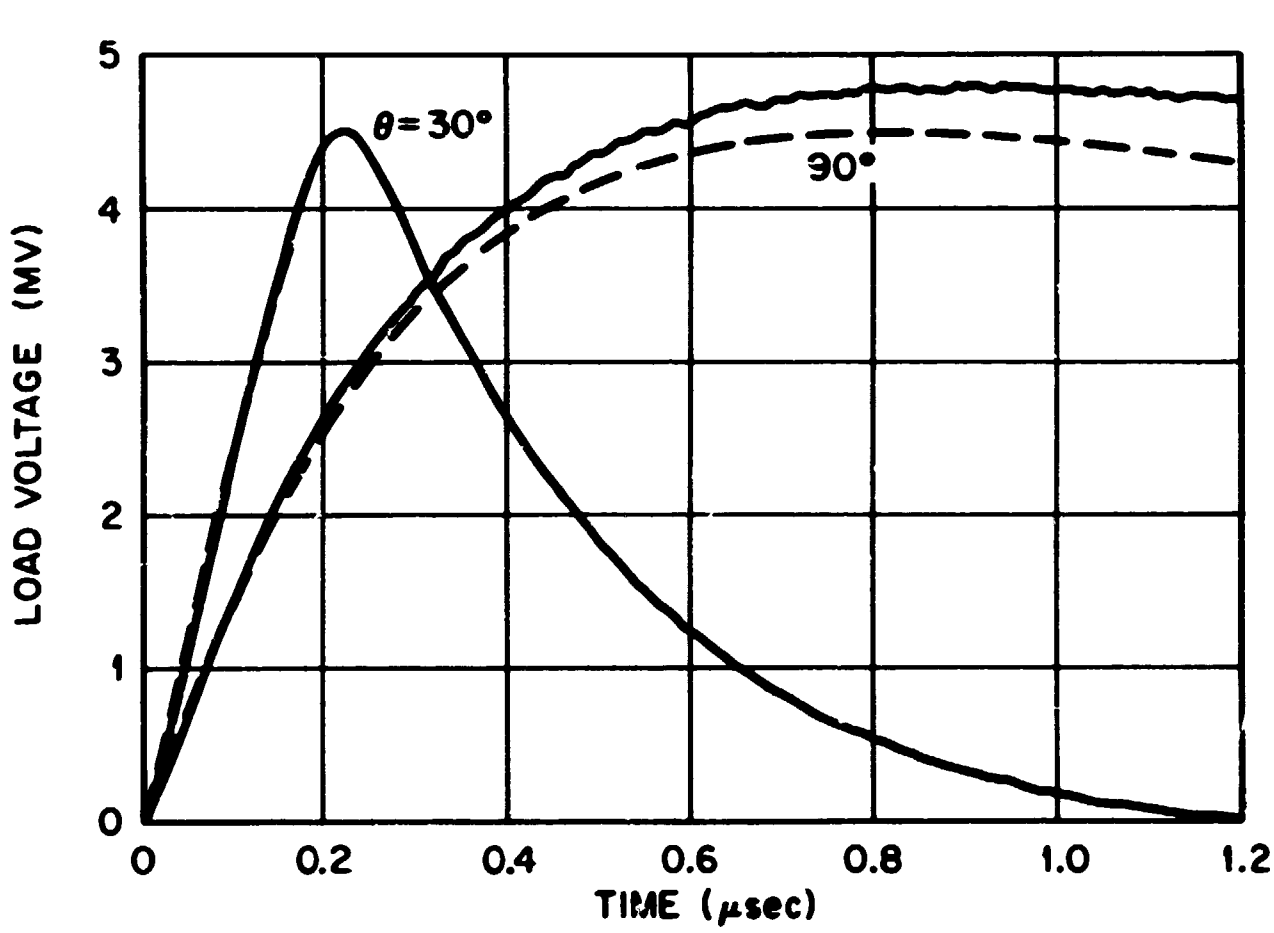

(*b*) RESPONSE TO THE LONG PULSE

Fig. 3.5. Early to Moderate Time Load Voltage Response.

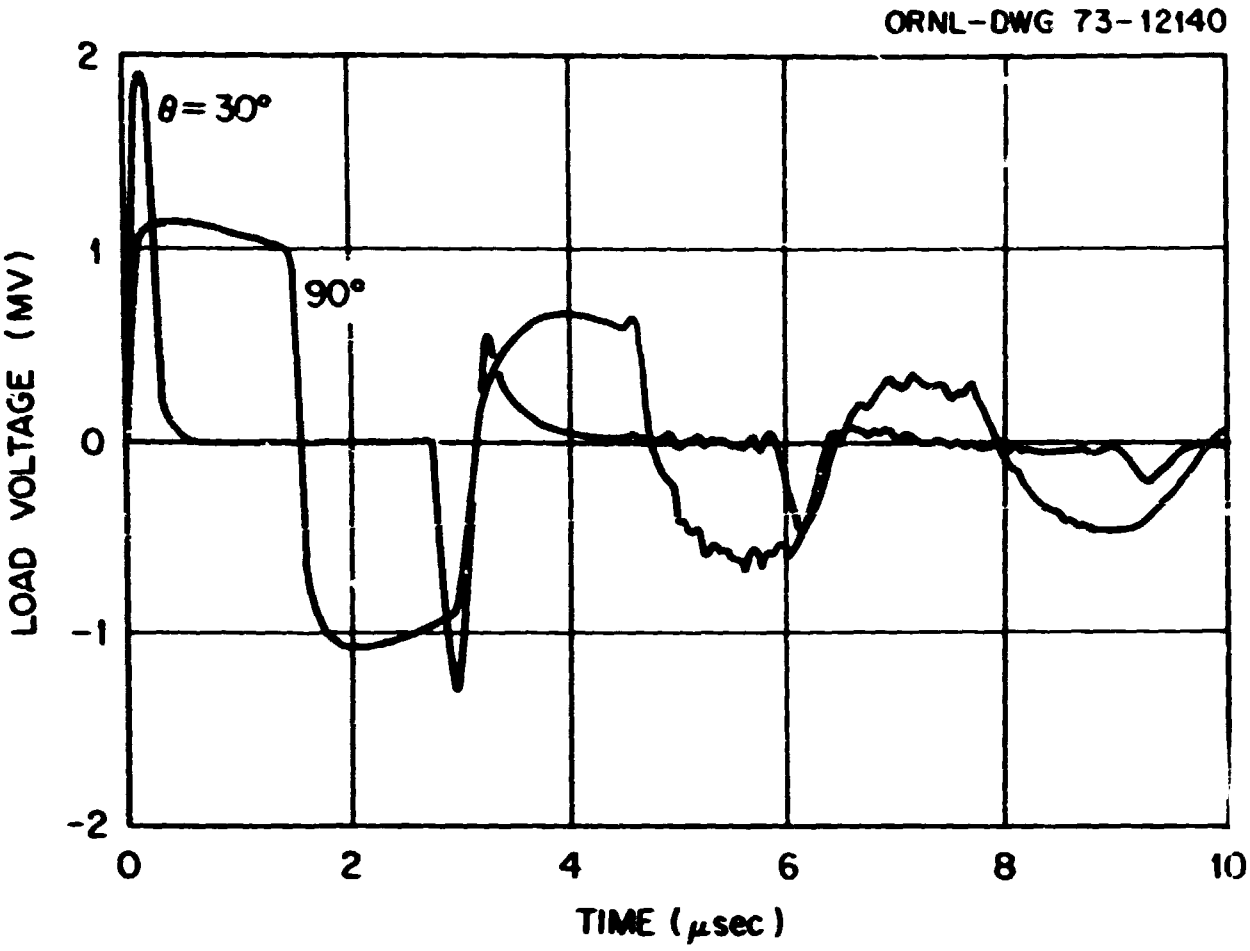

(a) RESPONSE TO THE SHORT PULSE

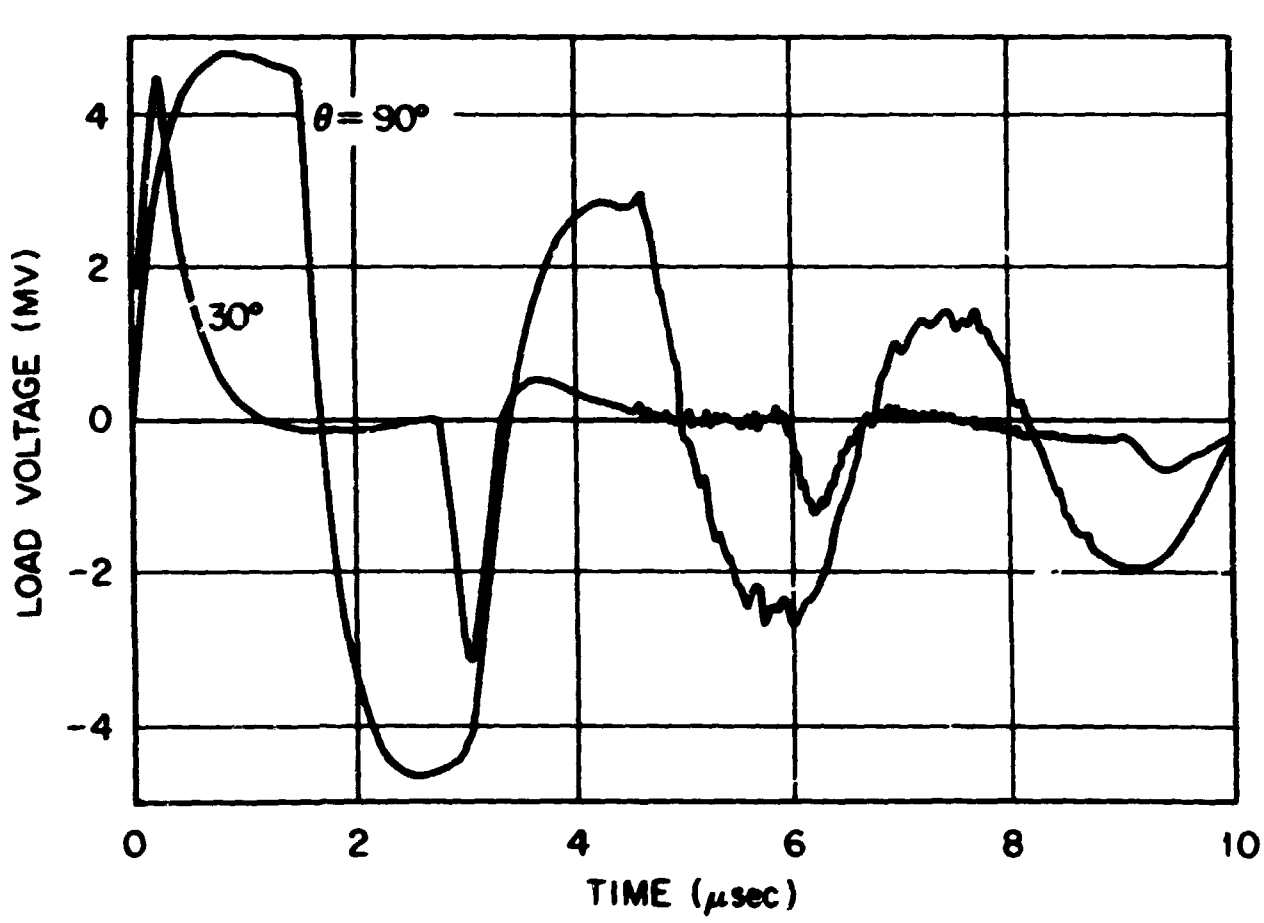

(b) RESPONSE TO THE LONG PULSE

Fig. 3.6. Moderate Time Load Voltage Response.

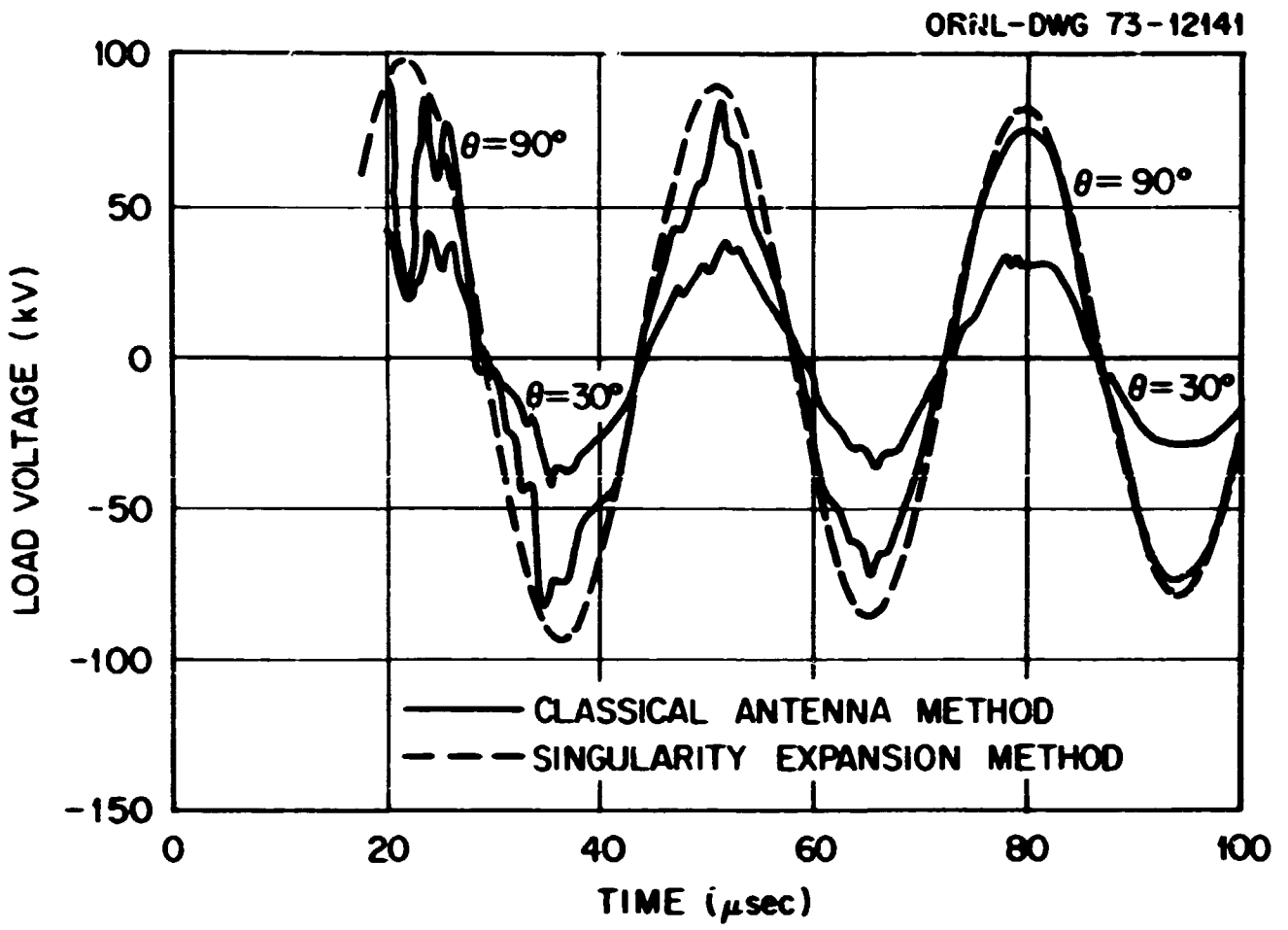

(*a*) RESPONSE TO THE SHORT PULSE

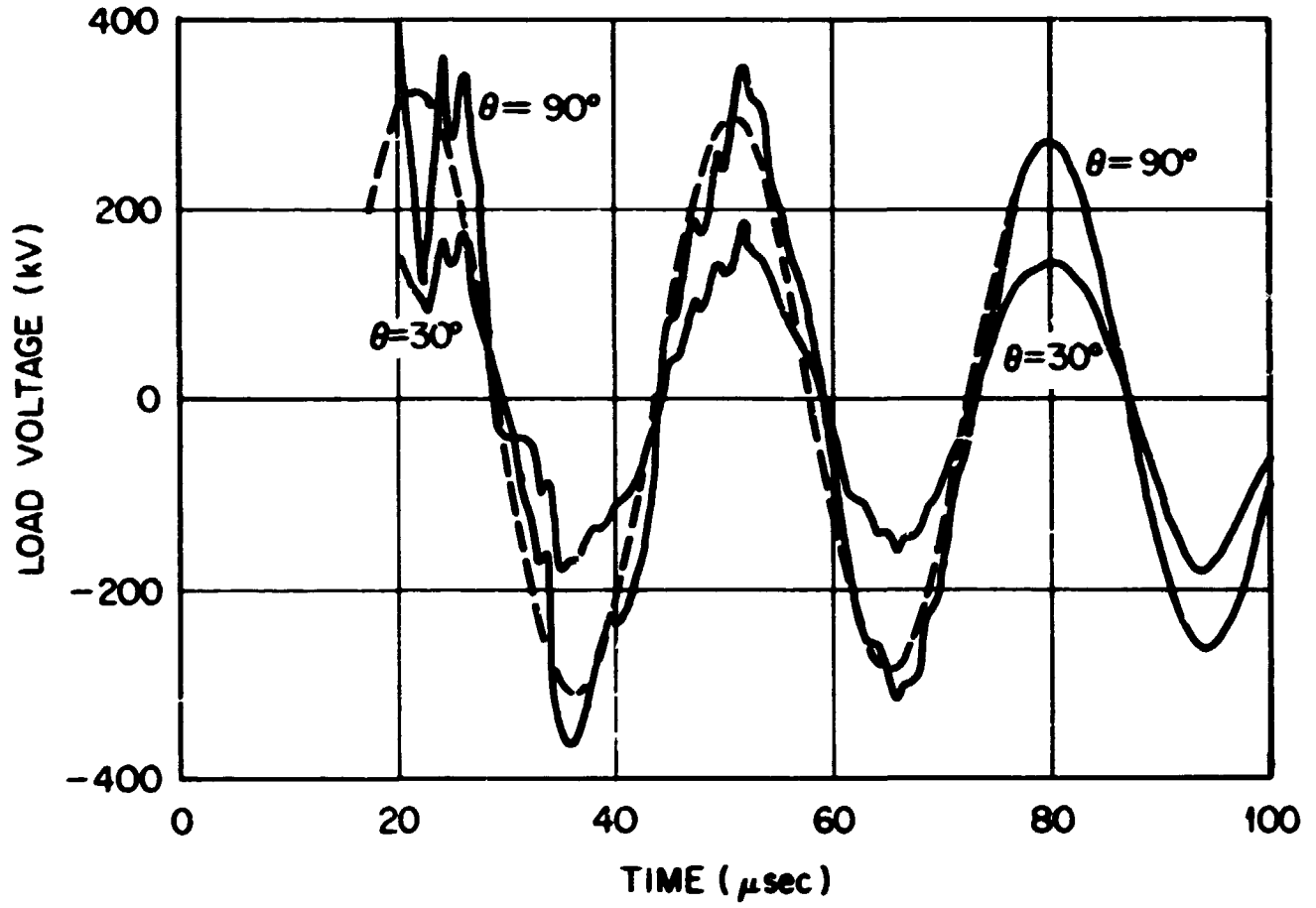

(*b*) RESPONSE TO THE LONG PULSE

Fig. 3.7. Late Time Load Voltage Response.

classical antenna method for times greater than 70 μsec. However, these errors were easily removed by averaging the high frequency oscillations introduced by the inverse Fourier program.

4. CONCLUSIONS

4.1 Comparison Among the Antenna Models

Our main reason for using a number of antenna models was to provide sufficient checks on the computed results. The very good agreement obtained in all cases indicates that there are no significant numerical errors present. Some adjustments were required. For example, to obtain the early time results of Figs. 3.1 and 3.4 the classical method required frequency domain values up to kh = 120. This includes approximately 75 antenna resonances and over 700 frequency points for the inverse Fourier transform.

The models describe the LF vertical radiator imperfectly, particularly in their treatment of the umbrella. Although the early and late time results should be quite accurate, the moderate time response of Figs. 3.3 and 3.6 could be in error since the models do not include the separate resonant effects associated with the physical lengths of the tower and the umbrella alone. Such error would likely be in the time behavior, the peak values of current and voltage are probably fairly accurate even for moderate time. The oscillatory wave associated with the umbrella is poorly coupled to the LF antenna's terminals and thus would have a small effect. The resonant effect of the physical tower height could decrease the first zero crossing time of the response by as much as 20 percent. However, the peak of the current and voltage will not be affected since the time of the first peak is sufficiently less than the first zero crossing time. Other deficiencies in the models include the assumptions of perfect conductivity for antenna and ground plane, treatment of load elements by lumped parameters, and neglect in all but the infinite antenna model of the gap between tower base and ground. Comparison of results shows this last error to be insignificant for the cases considered. The lumped parameter simplification, by neglecting capacitance in the feed line, might cause the early time voltage of Figs. 3.4 and 3.5 to be slightly too large. And finite conductivity would slightly reduce the computed currents and voltages.

4.2 Discussion of Results

LF vertical radiators respond quite dramatically to EMP from high altitude detonations. Peak currents calculated exceed 20 kA (Fig. 3.2) and peak load voltage is almost 5 MV (Fig. 3.5). Peak rate of rise is 500 kA/μsec (Fig. 3.1) and 30 MV/μsec (Fig. 3.4). These values can be compared with average peak lightning currents of 10-20 kA and rate of rise of 5-20 kA/μsec. The duration of current surges from lightning strokes would generally be longer than those induced by EMP. For these calculations we have not included any lightning arresters or other protective devices. Such devices would shorten the duration of EMP induced surges.

The effect of the angle of incidence θ is quite pronounced. The early time current and voltage at 30° is almost twice what it is at 90°, confirming the $\sin^{-1}\theta$ behavior. On the other hand, end effects occur sooner at 30°, reducing the low frequency content. Thus the late time behavior is greater for 90°. In general it will be true for long antennas that effects depending on initial rate of rise will be maximized for small θ, whereas effects that depend on total surge energy are maximized for broadside incidence.

REFERENCES

1. P. R. Barnes, "On the Response of an Infinitely Long, Perfectly Conducting, Cylindrical Dipole Anterna to an Electromagnetic Plane Wave Pulse," Interaction Note 157, published at the Air Force Weapons Laboratory (February 1974).

2. R. W. P. King, et.al., "The Electrically Short Antenna as a Probe for Measuring Free Electron Densities and Collision Frequencies in an Ionized Region," Journal of Research of the National Bureau of Standards - D. Radio Propagation, 65, 371 (1961).

3. T. T. Wu, "Theory of the Dipole Antenna and the Two Wire Transmission Line," Journal of Mathematical Physics, 4, 550 (1961).

4. L. C. Shen, T. T. Wu, and R. W. P. King, "A Simple Formula of Current in Dipole Antennas," IEEE Transactions on Antennas and Propagation, AP-16, 542 (1968).

5. L. C. Shen, "A Simple Theory of Receiving and Scattering Antennas," IEEE Transactions on Antennas and Propagation, AP-17, 112 (1970).

6. Carl E. Baum, "On the Singularity Expansion Method for the Solution of Electromagnetic Interaction Problems," Interaction Note 88, published at the Air Force Weapons Laboratory (11 December 1971).

7. Paul R. Barnes, The Analysis and Simulation of the Cylindrical Electric Dipole Antenna Response to EMP, ORNL-TM-4086 (September 1973).

8. W. J. Karzas and R. Latter, "Detection of the Electromagnetic Radiation from Nuclear Explosions in Space," Phys. Rev., 137, B1369 (1965).

9. D. B. Nelson, Effects of Nuclear EMP on AM Radio Broadcast Stations in the Emergency Broadcast System, ORNL-TM-2830 (1971). Obtainable from NTIS as AD 717319.

10. Henry Jasik, Ed., Antenna Engineering Handbook, Chapter 19, First Edition, McGraw-Hill (1961).

11. Paul R. Barnes, "On the Singularity Expansion Method As Applied to the Cylindrical Dipole Receiving Antenna," 1973 G-AP International Symposium, IEEE G-AP Proceeding, IEEE Catalogue No. 73 CHD 764-1AP (August 1973).

12. R. W. P. King, "Dipoles in Dissipative Media," Electromagnetic Waves, R. E. Langer, Ed., University of Wisconsin Press, Madison (1962), pp. 208-211.